Journal of Visualized Experiments

Simulating Imaging of Large Scale Radio Arrays on the Lunar Surface

--Manuscript Draft--

Article Type:	Invited Methods Article - JoVE Produced Video
Manuscript Number:	JoVE61540R1
Full Title:	Simulating Imaging of Large Scale Radio Arrays on the Lunar Surface
Section/Category:	JoVE Engineering
Keywords:	Radio Arrays, Radio Astronomy, Lunar, Interferometry, Simulations, Photoelectron Sheath, Imaging, Magnetospheric Emissions, Space Weather.
Corresponding Author:	Alexander Michael Hegedus, Ph.D. University of Michigan Ann Arbor, MI UNITED STATES
Corresponding Author's Institution:	University of Michigan
Corresponding Author E-Mail:	alexhege@umich.edu
Order of Authors:	Alexander Michael Hegedus, Ph.D.
Additional Information:	
Question	**Response**
Please indicate whether this article will be Standard Access or Open Access.	Open Access (US$4,200)
Please indicate the **city, state/province, and country** where this article will be **filmed**. Please do not use abbreviations.	Ann Arbor, MI USA

JoVE Cover Letter

Author Biography

Alexander Hegedus is a Postdoctoral Research Fellow at the Climate and Space Sciences and Engineering Department at University of Michigan. He earned his dual degree PhD in Atmospheric Oceanic and Space Sciences & Scientific Computing from University of Michigan in 2019. He received his Bachelors in Mathematics & Computer Science in 2014 from Alma College, and his Masters in Atmospheric , Oceanic, and Space Sciences from University of Michigan in 2016. As a graduate student Alex worked with the ground based radio interferometer Long Wavelength Array, conducting various pulsar measurements. He interned at JPL in the summer of 2016 & 2017, working with multiple teams on different space based array concepts. His presentation Simulating 3D Spacecraft Constellations for Low Frequency Radio Imaging won an Outstanding Student Paper Award (OSPA) at the American Geophysical Union Fall Meeting in 2016. Alex is centrally involved in SunRISE, a recently funded NASA Heliophysics Mission of Opportunity that will launch 6 satellites into GEO orbit in 2023 to create the first synthetic aperture in space. His research interests include Heliophysics, Radio Astronomy, Scientific Computing, and Machine Learning.

TITLE:

Simulating Imaging of Large Scale Radio Arrays on the Lunar Surface

AUTHORS AND AFFILIATIONS:

Alexander M. Hegedus

Department of Climate and Space Sciences and Engineering, University of Michigan, Ann Arbor, MI, USA

Corresponding Author:
Alexander M. Hegedus (alexhege@umich.edu)

KEYWORDS:

Radio Arrays, Radio Astronomy, Lunar, Interferometry, Simulations, Photoelectron Sheath, Imaging, Magnetospheric Emissions, Space Weather

SUMMARY:

A simulation framework for testing the imaging capabilities of large-scale radio arrays on the lunar surface is presented. Major noise components are discussed, and a software pipeline is walked through with details on how to customize it for novel scientific uses.

ABSTRACT:

In recent years there has been a renewed interest in returning to the Moon for reasons both scientific and exploratory in nature. The Moon provides the perfect training ground for building large scale bases that one may apply to other planets like Mars. The existence of a radio quiet zone on the lunar far side has promise for early universe studies and exoplanet searches, while the near side provides a stable base that may be used to observe low frequency emissions from Earth's magnetosphere that may help gauge its response to incoming space weather. The construction of a large-scale radio array would provide large scientific returns as well as acting as a test of humanity's ability to build structures on other planets. This work focuses on simulating the response of small to large-scale radio arrays on the Moon consisting of hundreds or thousands of antennas. The response of the array is dependent on the structure of the emission along with the configuration and sensitivity of the array. A set of locations are selected for the simulated radio receivers, using Digital Elevation Models from the Lunar Orbiter Laser Altimeter instrument on Lunar Reconnaissance Orbiter to characterize the elevation of the receiver locations. A custom Common Astronomy Software Applications code is described and used to process the data from the simulated receivers, aligning the lunar and sky coordinate frames using SPICE to ensure the proper projections are used for imaging. This simulation framework is useful for iterating array design for imaging any given scientific target in a small field of view. This framework does not currently support all sky imaging.

INTRODUCTION:

The field of radio astronomy began in 1932 with the accidental detection of galactic radio emission by Karl G. Jansky[1] at 20 MHz, in a range now commonly called the low frequency radio. Ever since then, radio astronomy has grown rapidly, catching up with higher frequency optical observations that have been going on for centuries longer. Another breakthrough was the utilization of radio interferometry, where groups of antenna separated by large distances are used to create a synthetic aperture, providing a way to scale up the sensitivity and resolution of radio observations[2,3]. This can intuitively be thought of as an extension of the regular resolution formula for optical observations:

$$\theta_{HPBW} = 1.22\,\frac{\lambda}{D} \quad (1)$$

For an observing dish of size D meters, and an observing wavelength of λ meters, Θ_{HPBW} is the angular size in radians of the Half Power Beam Width (HPBW), defining the resolution on the sky. This process of synthesizing a fraction of a large full dish with only scattered points across a mostly empty area is also called aperture synthesis. In the realm of radio interferometry, the resolution of an array is determined by the furthest distance between any two receivers in the array, and this distance is used as D in Equation 1.

The mathematics behind interferometry has been well documented in classic texts like Thompson's Interferometry and Synthesis in Radio Astronomy[3]. The basic insight can be communicated informally as "(for planar arrays observing a small field of view) the cross correlation of signals between any 2 receivers (a *visibility*) will yield information about a 2D Fourier coefficient of the sky brightness pattern." What Fourier mode is sampled depends on the separation of the receivers (the *baseline*), normalized by the observing wavelength. Receivers that are further apart (in the standard UVW coordinate system oriented towards the imaging target) sample higher spatial frequency features, yielding higher resolution details at smaller scales. Conversely, receivers that are close together in the same UVW frame sample lower spatial frequencies, giving information of larger scale structures at a lower resolution.

For the lowest radio frequencies, free electrons in Earth's ionosphere prevent radio waves below 10 MHz from travelling from space to the ground, and vice versa. This so-called "ionospheric cutoff" has long prevented ground-based observations of the sky for this frequency range. The obvious answer to this limitation is to put radio receivers into space where they can record data free of the influence of Earth's atmosphere and free electrons in its ionosphere. This has been done before with single antennas on spacecraft like Wind[4] and STEREO[5], which have revealed many astrophysical processes that produce emissions in this low frequency radio range. This includes emissions from the interactions of electrons with the Earth's magnetosphere, electron acceleration from solar eruptions, and from the galaxy itself. Single antenna observations can measure the total flux density of such events, but cannot pinpoint where the emission is coming from. In order to localize this low frequency emission and make images in this frequency regime for the first time, many antennas will have to be sent to space and have their data combined to make a synthetic aperture.

Doing this would open a new window through which humankind can observe the universe, enabling a number of scientific measurements that require images of the sky in these lowest frequencies. The Moon is one possible site for a synthetic aperture in space, and it comes with pros and cons when compared to free flying orbiting arrays. The lunar far side has a unique radio quiet zone that blocks all of the usual interference coming from man-made signals, while the near side provides a static place for Earth observing arrays, and if constructed at the lunar sub-Earth point, the Earth will always be at the zenith of the sky. With a static array, it is easier to obtain short baselines to measure large scale emissions, as they are in no danger of colliding, unlike free flying arrays. The drawbacks of a lunar array are chiefly difficulties in cost and power. A large-scale array on the Moon would require a substantial amount of infrastructure and money, while smaller orbiting arrays would require far fewer resources. There is also the issue of power; most places on the Moon are exposed to sufficient sunlight for solar power generation for 1/3 of each lunar day. Surviving the large swings in temperature from lunar day to night is also an engineering concern. Putting aside these difficulties, there is still the problem of making sure that the proposed array design is suitable for its specified science target(s). The response of any given array is dependent on the structure of the emission being observed along with the configuration and sensitivity of the array.

Several conceptual arrays to go on the lunar surface have been drawn up over the decades. Early designs were not the most detailed, but still recognized the scientific advances that could be attained by such arrays[6,7,8,9,10]. More arrays have also been put forth in recent years, some of which, like FARSIDE[11], DEX[12], and DALI[13] seek to measure the absorption troughs of the redshifted neutral hydrogen 21-cm signal in the 10-40 MHz range to probe the so called "Dark Ages" and constrain cosmological models of the early universe. Others like ROLSS[14] call out tracking bright solar type II radio bursts far into the heliosphere to identify the site of solar energetic particle acceleration within coronal mass ejections as their compelling science case. Smaller scale arrays have also been described like the 2-element interferometer RIF[15], which would use a single lander and a moving rover to sample many baselines as it moves outward from the lander. RIF focuses on the ability to make a sky map of these low frequencies for the first time, and calculates the UV coverage and synthesized beam for integrated observations.

Space-based radio arrays could also enable low frequency imaging of distant radio galaxies to determine magnetic fields and astrometric measurements[16]. Low frequency images of these bodies would provide a more complete picture of the physics governing these systems, in particular yielding synchrotron emission data for the lower end of the electron energy distribution. There are also a range of various magnetospheric emissions that occur at these low frequencies, providing both global (constant synchrotron emission) and local (bursts, auroral kilometric radiation) signatures of electron dynamics that are not detectable from the ground[17]. The brightest recorded emissions of these types have come from Earth and Jupiter, as these are the nearest planets with strong magnetospheres. However, arrays with sufficient sensitivity and resolution could observe magnetospheric emission from other outer planets, or even extrasolar planets[18]. This topic in particular was called out as an area of interest at the recent Planetary Sciences Vision 2050 workshop.

This work focuses on simulating the response of radio arrays on the Moon consisting of anywhere from just a few antennas, to hundreds or thousands of antennas. This simulation framework is useful for iterating array design for imaging any given scientific target in a small field of view (a few square degrees) but does not currently support all sky imaging. Accurate estimates of the predicted brightness maps along with realistic noise profiles must be used to ensure that a given array size/configuration is sufficient to observe the target to a certain noise level or resolution. The geometry of the array must also be known to a high degree so that the baselines are computed accurately to enable correct imaging of the data. Currently, the best maps of the Lunar surface are Digital Elevation Models (DEMs) from Lunar Reconnaissance Orbiter's (LRO's)[19] Lunar Orbiter Laser Altimeter (LOLA)[20]. The simulation pipeline accepts longitude latitude coordinates for each receiver and interpolates the elevation at these points from existing DEMs to calculate the full 3D position.

From these coordinates the *baselines* are computed and inserted into a Common Astronomy Software Applications (CASA)[21] Measurement Set (MS) file. The MS format can be used with many existing analysis and imaging algorithms, and holds information about the array configuration, visibility data, and alignment with the sky. However, many of these software routines are hard coded to work with arrays that rotate with the Earth's surface, and do not work for orbiting or Lunar arrays. To circumvent this, this pipeline manually calculates the baselines and visibilities for a given array and imaging target, and inserts the data into the MS format. The SPICE[22] library is used to correctly align the lunar and sky coordinate systems and track the motions of the Moon, Earth, and Sun.

The simulation framework described here follows Hegedus et al.[17], and the software is archived by the University of Michigan library in the Deep Blue archive[23], stored at https://deepblue.lib.umich.edu/data/concern/data_sets/bg257f178?locale=en. The following section will describe the requirements for this software, and walk through the process of forming an array, setting the appropriate noise levels, feeding the array a simulated truth image of the targeted emission, and simulating the array's noiseless and noisy reconstructions of the emission using a CASA script.

PROTOCOL:

1. Software setup

1.1. First, go to https://deepblue.lib.umich.edu/data/concern/data_sets/bg257f178?locale=en and download the software package. This software has only been tested in a UNIX environment, and may not fully function in other environments. The README in this package will help guide one through the rest of the software needed and its uses.

1.2. Make sure python 2.7 or greater is installed. A link is provided in the README. Several common python libraries are also needed including numpy, matplotlib, pylab, scipy, subprocess, ephem, and datetime.

1.3. Make sure CASA 4.7.1 or greater is installed. A link in provided in the README.

1.4. Make sure gcc 4.8.5 or greater is installed. A link is provided in the README.

1.5. Make sure the C toolkit for SPICE is installed. This software is used to align different astronomical reference frames and track the relative positions of planets, moons, and satellites. A link to download this software is also included in the README.

1.5.1. Download several kernels that contain information on astronomical and lunar reference frames, as well as the orbital dynamics of the Moon, Earth, and Sun. The specific kernels needed are listed in the README alongside a link of where to download them.

1.6. Obtain the final prerequisite data needed: Digital Elevation Models (DEMs) of the lunar surface created from LRO LOLA measurements. The specific file needed is listed and linked in the README.

2. Creating the array configuration

2.1. Customize the createArrayConfig.py script.

2.1.1. Choose the configuration of the array by providing a list of Longitude and Latitude coordinates for each antenna.

NOTE: The script is currently formatted for a 10 km diameter array with 1024 elements, 32 arms with 32 log space spaced antenna each, using a constant factor to convert between meters and degrees of longitude/latitude near 0 degrees latitude. The site of the array, (-1.04°, -0.43°), was chosen because it is the center of the 10x10 km patch with the lowest elevation variation (σ =5.6 m) close to the sub-Earth point (0°, 0°) in the Moon ME frame.

2.1.2. Change the lunarPath variable in the script to reflect the new download location of the Digital Elevation Model containing the elevation data of the lunar surface.

2.2. Run the createArrayConfig.py script with "python createArrayConfig.py". This will use the lunar Digital Elevation Model to solve for the elevation at each longitude and latitude for each antenna. Save the longitude, latitude, and elevation to files and print to the screen for easy copying and pasting into the next script. Make figures showing the array configuration on top of the local lunar topography (**Figure 1**).

3. Using SPICE to align coordinates

3.1. Customize the eqArrOverTimeEarth.c script.

3.1.1. Take the output from the previous script, the Longitude, Latitude, and elevation of each antenna and copy them over into the corresponding lists in the script, also updating the variable 'numsc' with the number of receivers and corresponding coordinates.

NOTE: Since C does not have dynamic array allocation, there was no easy way to flexibly read in the data automatically, so manual copying must be done.

3.1.2. 3.1.2 Update the lunar_furnsh.txt included in the package with the new path names for the required frame and ephemeris files.

3.1.3. Specify what set of dates to observe on. This will inform the ephemerides within SPICE to accurately track where the Earth and Sun are in relation to the defined array for those dates. In the script currently 48 dates occurring roughly weekly over the year 2025 are selected.

3.1.4. Specify the targeted area of the sky for the array to track and image. Currently the script saves the RA Dec of the Earth as seen from the lunar surface, but one may easily just put in static RA Dec coordinates instead.

3.2. Compile the eqArrOverTime.c script

3.2.1. Compile the script using the gcc command in the comment at the top of the script. It will be something like "gcc eqArrOverTimeEarth.c -o eqArrOverTimeEarth -I/home/alexhege/SPICE/cspice/include /home/alexhege/SPICE/cspice/lib/cspice.a -lm -std=c99". Change the paths to reflect where the cspice libraries are located.

3.3. Run the eqArrOverTime executable with "./eqArrOverTime". This should result in a number of files each with a set of variables in them. Most important are the XYZ position of each antenna in J2000 coordinates, and the Right Ascension and Declination (RA and Dec) coordinates of the targeted area in the sky (currently those of the Earth from the Moon's perspective). The output variables are saved to .txt files containing the data for all the requested dates.

4. Using CASA to simulate array response

4.1. Customize the LunarEarthPicFreqIntegration.py script.

4.1.1. Specify the observing frequency for the array to make an image at. This is currently set to 0.75 MHz.

4.1.2. Specify a CASA compatible truth image (or create from a .fits image file) with Jansky/pixel values for the array to reconstruct (e.g., **Figure 2**). Constants (res, res1, width, arcMinDiv) in the code will need to be changed to reflect the size and resolution of the input truth image.

NOTE: The current used images estimates of synchrotron emission that are 400x400 pixels, with each pixel being 0.38 degrees. Each pixel has a Jansky/pixel value, specifying the radio brightness coming from that area in the sky. The .truth files also encode where in the sky they are, taking the RA Dec coordinates from the previous script. This results in an internal coordinate system centered on those coordinates, with every pixel value having an assigned sky position based off the resolution of the input image.

4.2. Run the LunarEarthPic.py script. Commented at the top of the script are examples on how to run the script. The following command is one example on how to run the script from the command line:

“nohup casa --nologger --nologfile --nogui --agg -c LunarEarthPicFreqIntegration.py -outDir . -correlate True -numSC 1024 | tee earth.out &”

The -numSC flag is used to inform the code how many antenna/receivers are being used, and helps unpack the data from the .txt files containing the receiver coordinates.

NOTE: The antenna baseline vector, measured in units of the observing wavelength (λ), has length D_λ and components (u, v, w) = (Δx,Δy,Δz)/λ . The pipeline then calculates the visibilities, or observed cross correlated voltages for each pair of antennas. Here the small field of view approximation is used to calculate the visibilities, following the standard formula from Thompson et al.[2] for an infinitesimal bandwidth at frequency ν.

$$V_\nu(u, v, w) = \iint \frac{A_\nu(l,m) I_\nu(l,m)}{\sqrt{1-l^2-m^2}}\, e^{-2\pi i(ul+vm+w(n-1))} dl dm \quad (2)$$

The sky coordinates of the target the array is imaging is deemed the phase center, to which the z, or w, axis of the frame is pointed. (l, m, n) are the direction cosines from the (U, V, W) coordinate system. The sky brightness pattern around the source under observation is $I_\nu(l, m)$. Spectral flux density is often presented in the derived unit 1 Jansky (Jy) = 10−26 W/m^2/Hz. Spectral brightness is simply Jy/steradian to represent the amount of flux coming from a particular area in the sky. $A_\nu(l, m)$ is the normalized antenna primary beam pattern, or how sensitive it is to radiation coming from that point in the sky.

This script calculates the antenna separations in the appropriately projected reference frame from the coordinates output from the previous script. It then uses Equation 2 to calculate the visibility data for each pair of antenna. The resulting visibilities are stored alongside the baselines in a CASA Measurement Set file (.ms). This MS file is the primary output of this script.

5. Imaging the data – noiseless and noisy

5.1. Customize the noiseCopies.py script.

5.1.1. Set the System Equivalent Flux Density (SEFD), referred to as avNoise in the script. The SEFD is a convenient way to talk about the total noise of a radio antenna since it ties in both the system temperature and the effective area, and provides a way to directly compare the signal and the noise. It is currently set to 1.38e7 Jansky, which is an optimistic noise level for 0.75

MHz.

NOTE: For the low frequency radio regime, there are three main sources on constant noise: amplifier noise, quasithermal noise from free electrons (estimated by Meyer-Vernet et al.[24] to be 6.69e4 Jy at 0.75 MHz, using a electrically short dipole approximation), and Galactic background radiation from the Milky Way (estimated by Novacco & Brown[25] to be 4.18e6 Jansky at 0.75 MHz for the full sky, of which a lunar array will only see some portion). This optimal noise level of 1.38e7 Jy assumes that amplifier noise dominates the other terms. See Hegedus et al. for a more detailed discussion.

5.1.2. Set the bandwidth being integrated over in variable 'noise' line 200. Set to 500 kHz.

5.1.3. Set the integration time in variable 'noise' line 200.

5.2. Run the noiseCopies.py script with "nohup casa --nologger --nologfile --nogui --agg -c noiseCopies.py | tee noise.out &".

5.2.1. The script will first create an image from the noiseless visibility data, calling standard radio astronomy algorithm CLEAN[26] to create an image like **Figure 3**.

5.2.2. The script will then create copies of the MS and add the appropriate noise level to the complex visibility data and image it using CLEAN. The script currently makes images for a range of integration times up to 24 hours and over several robust weighting scheme values. Depending on the configuration of the array, image quality may vary with the choice of data weighting schemes. These noisy images will look something like **Figure 4**, which used an integration time of 4 hours.

NOTE: The noise is added with standard Signal to Noise formulas. From Taylor[2] the interferometric noise for a single polarization is

$$\sigma = \frac{SEFD}{\eta_s\sqrt{N_{ant}(N_{ant}-1)\Delta\nu\Delta t}} \quad (3)$$

Here, η_s is the system efficiency or correlator efficiency, which has been set to a conservative value of 0.8. N_{ant} is the number of antennas in the array ($N_{ant} = 2$ for each individual visibility), $\Delta\nu$ is the bandwidth being integrated over in Hz, and Δt is the integration time in seconds.

REPRESENTATIVE RESULTS:

Following the software pipeline should be fairly straightforward, and it should be obvious that each step is working as it should. Running createArrayConfig.py from step 2 should create a figure resembling **Figure 1**, where configuration of the defined array is plotted on top of the local topography of the lunar surface, as derived from the LRO LOLA derived Digital Elevation Model.

Step 3 should give key output files eqXYZ_EarthCentered.txt, RAs.txt, and Decs.txt, among others. Examples of these files are located in the downloaded package.

Step 4 should create a truth image that is similar to **Figure 2**, which is then used to calculate the visibility data. It should also output a CASA Measurement Set (.ms) file that one may browse with the usual CASA command of casabrowser to see that both the baselines and visibility data were calculated and saved.

Step 5 should output figures similar to **Figure 3 and 4** for the noiseless and noisy images respectively. The noisy images should look less clear than the noiseless image.

FIGURE AND TABLE LEGENDS:

Figure 1: Configuration of the array over elevation map of the lunar surface. This is an example array configuration consisting of a logarithmically spaced circular array over 10 km. The configuration has 32 arms of 32 logarithmically spaced antenna for a total of 1024 antenna. The site of the array, (-1.04°, -0.43°) was chosen because it is the center of the 10x10 km patch with the lowest elevation variation (σ =5.6 m) close to the sub-Earth point (0°, 0°) in the Moon Mean Earth (ME) frame. The elevation data was obtained from a Digital Elevation Map derived from LRO LOLA measurements. This figure was taken from Hegedus et al.[13].

Figure 2: Truth image of synchrotron emission from radiation belts at lunar distances. This is an example of a science target for the array to image. The recovered image is then compared to this input to determine the performance of the array. The brightness map was created from Salammbô electron simulation data and run through a calculation for determining the synchrotron emission that would be observed at lunar distances. The 1.91° Earth is added in for a scale indicator. This figure was taken from Hegedus et al.[13].

Figure 3: Noiseless response of 10 km diameter array to input truth image. This is one of the outputs from Step 5, applying standard radio astronomy imaging algorithm CLEAN, using a Briggs weighting scheme with a robustness parameter of −0.5. This figure was taken from Hegedus et al.[13].

Figure 4: Noisy response of 10 km diameter array to input truth image. This is one of the outputs from Step 5, applying standard radio astronomy CLEAN, using a Briggs weighting scheme with a robustness parameter of −0.5. For this image, a System Equivalent Flux Density of 1.38e7 Jansky was used, an integration bandwidth of 500 kHz, and an integration time of 4 hours. The noise was also reduced by a factor of 16 to simulate the response of a 16K antenna array instead of a 1K antenna array. This figure was taken from Hegedus et al.[13].

DISCUSSION:

Each step of the simulation pipeline is necessary and feeds into the next, taking an array configuration on the lunar surface, aligning the reference frame correctly to orient the array to the target area in the sky, calculating the visibility data, adding the appropriate noise levels, and running imaging algorithms on the resulting data.

For each step, customizations may be made. In step 2, the user defined array configuration may be any list of longitudes and latitudes. This then feeds into the SPICE script in step 3, where one may choose the exact time of the planned measurements, as well as where in the sky the array should be focused. In step 3, one can specify the simulated truth emission that the array is attempting to image by providing a suitable CASA .truth file. Then in step 4 one may change the expected level of noise depending on the observing frequency and expected hardware capabilities. This set of codes constitutes a flexible simulation framework that may be used to iterate array design for any number of uses, depending on the targeted science. These codes can all be run on an average laptop or workstation, though computation time increases with number of antennas. The slowest parts of the process are predicting the visibilities, followed by imaging. For small arrays, the entire process can be done in minutes, while for larger arrays of a few hundred or thousand receivers, hours or days may be needed.

Some next steps that could be taken with this pipeline to increase its realism include adding a channel-dependent foreground removal system. This requires building up a global sky model, dominated at low frequencies by galactic synchrotron emission and a few bright sources like Cas A, tracking which part of the sky is visible to the receivers, and convolving that brightness pattern with the primary beam, with the phase center of the array aligned towards the imaging target. For longer integration times, tracking the apparent motion of the sky is also an issue. Another improvement that could be added is a transient event/radio frequency interference (RFI) flagging system that can remove flagged channels from normal imaging, and send them to a specialized pipeline that images and characterizes the flagged data. This transient event pipeline could then use special algorithms like uvmodelfit that can take advantage of the high signal to noise ratio of these events to characterize them better than the normal resolution of the array[27].

There are also additional effects that need to be taken into account for a full array calibration, one of which is mutual coupling. As discussed in Ellingson[28], this can lead to a decrease in sensitivity in arrays if they have receivers that are within a few wavelengths of each other. This is seen in a decrease in sensitivity for the array, or equivalently, an increase in the SEFD. This is especially true for beams greater than 10 degrees away from zenith. The example array in this work targets Earth, which is always near zenith by design, so mutual coupling should not affect this particular imaging target, but studies of the SEFD over the full range of elevation angles and frequencies will need to be done in commissioning for any real array to unlock its full potential. Another shortcoming of this array simulation pipeline lies in the imperfect lunar surface maps used. DEMs from LRO LOLA measurements have at best a resolution of 60x60 meters/pixel in the 512 pixels/degree maps. One can interpolate these data for simulated arrays, but for real arrays there will need to be a commissioning/calibration period where sources with a known position will be used to determine the relative separations between all the antenna to high precision. Possible calibration sources include Cas A, periodic low frequency emission from Jupiter or Earth, or potentially the Lunar Gateway[29].

There is also the response of the lunar surface to consider. There is a layer of lunar topsoil called the regolith that acts like a lossy dielectric that can reflect incoming emission with some efficiency, above the lunar bedrock which can also reflect incoming emission with some better efficiency[30,31]. This response is dependent on the ambient temperature and incoming frequency, as well as the chemical composition of the regolith. Studies[30,31] have found that at lower temperatures below 100 K, the regolith is nearly transparent to radio emission, and reflection occurs at the bedrock level with a reflection coefficient of around 0.5-0.6. At higher temperatures 150-200 K, the regolith can absorb emission and reflect incoming radiation at the surface with a reflection coefficient of around 0.2-0.3. At temperatures above 200 K, it is found that the dielectric properties of the regolith are diminished, and variation from reflection can be ignored. These effects can reduce the effective area of the array, reducing sensitivity and requiring longer integration times. This effect can be modeled with electromagnetic simulation software packages such as NEC4.2[32] given models of relative permittivity/dielectric constant as a function of lunar depth. This will output the SEFD of a receiver for a given frequency, which can be given to the array simulation pipeline to calculate the correct noise to add to the simulated signal. Adding a grounding grid between the receiver and the lunar surface may help diminish the effect of reflected waves, but adds its own set of complications in the form of deployment.

Many of the hypothetical or fuzzy details around the implementation of a radio receiver on the lunar surface will finally solidify into reality with recent funding of single low frequency antenna projects like Radio wave Observations on the Lunar Surface of the photoElectron Sheath (ROLSES) and the Lunar Surface Electromagnetics Experiment (LuSEE)[33]. LuSEE was recently funded by NASA as part of the Commercial Lunar Payload Services program. Both suites of antenna will consist mainly of flight spares for past instruments like STEREO/WAVES or PSP FIELDS and are planned for a 2021 delivery. Measurements from these receivers will finally solidify the level of quasithermal noise from the photoelectron sheath from ionized dust on the lunar surface and how it changes over the course of a lunar day. These measurements will also characterize the level of reflection and absorption from the lunar surface, and quantify how it changes the SEFD of the receiver. They will also provide statistics on the number of transient events or RFI that are received on the lunar surface. These missions will pave the way for arrays of antennas that will finally be able to make a multitude of novel scientific observations such as low frequency emission from solar radio bursts, far away galaxies, and planetary magnetospheres. The simulation pipeline described in this work provides a flexible way to iterate the design of these future arrays for a variety of scientific targets.

ACKNOWLEDGMENTS:

Thanks to the Lunar Reconnaissance Orbiter (LRO) and Lunar Orbiter Laser Altimeter (LOLA) teams for providing the Lunar Digital Elevation Maps. This work was directly supported by the NASA Solar System Exploration Research Virtual Institute cooperative agreement number 80ARC017M0006, as part of the Network for Exploration and Space Science (NESS) team.

DISCLOSURES:

The authors have nothing to disclose.

REFERENCES:

1. Jansky, K. G. Directional studies of atmospherics at high frequencies. *Proceedings of Institute of Radio Engineers*. **20**, 1920 (1932).
2. Taylor, G. B., Carilli, C. L., Perley, R. A. *Synthesis Imaging in Radio Astronomy II*, Vol. 180 of *Astronomical Society of the Pacific Conference Series* (1999).
3. Thompson, A. R., Moran, J. M., Swenson, G. W. *Interferometry and synthesis in radio astronomy*. New York, Wiley-Interscience (1986).
4. Bougeret, J. et al. WAVES: The radio and plasma wave investigation on the Wind spacecraft. *Space Sciencce Reviews.* **71**, 231–263 (1995).
5. Bougeret, J. et al. S/WAVES: The Radio and PlasmaWave Investigation on the STEREO Mission. *Space Science Reviews*. **136** (1), 487–528 (2008).
6. Burke B. F. Astronomical Interferometry on the Moon, *Lunar bases and space activities of the 21st century* (A86-30113 13-14), ed. W. W. Mendell, Lunar and Planetary Institute, USA, 281-291 (1985).
7. Burns, J. O., A moon-earth radio interferometer, *Lunar bases and space activities of the 21st century* (A86-30113 13-14), ed. W. W. Mendell, Lunar and Planetary Institute, USA, 293-300 (1985).
8. Douglas, J. N. et al. A very low frequency radio astronomy observatory on the moon, *Lunar bases and space activities of the 21st century* (A86-30113 13-14), ed. W. W. Mendell, Lunar and Planetary Institute, USA, 301-306 (1985).
9. Damé, L. et al. Solar interferometric imaging from the moon. *Advances in Space Research*. **14** (6), 49-58, (1994).
10. Bely P. Y. et al. Very Low Frequency Array on the Lunar Far Side. Technical Report, *ESA SCI* (97)2, 1997.
11. Burns, J. O. et al. FARSIDE: A Low Radio Frequency Interferometric Array on the Lunar Farside. *Bulletin of the American Astronomical Society*, **51** (7), no. 178 (2019)
12. Klein-Wolt, M. et al. Dark ages EXplorer, DEX, A white paper for a low frequency radio interferometer mission to explore the cosmological Dark Ages. *L2, L3 ESA Cosmic Vision Program* (2013).
13. Lazio T. J. et al. The Dark Ages Lunar Interferometer (DALI) and the Radio Observatory for Lunar Sortie Science (ROLSS). *Bulletin of the American Astronomical Society*. **41**, 344 (2009).
14. MacDowall, R.J. et al. A Radio Observatory on the Lunar Surface for Solar studies (ROLSS). *arXiv e-prints.* (2011).
15. Aminaei, A. et al. Basic radio interferometry for future lunar missions. *2014 IEEE Aerospace Conference Proceedings*. Big Sky, MT. 1-19 (2014).
16. Belov, K. et al. A space-based decametric wavelength radio telescope concept. *Experimental Astronomy*. **46** (2), 241–284 (2018).
17. Hegedus, A. M. et al. Measuring the Earth's synchrotron emission from radiation belts with a lunar near side radio array. *Radio Science*. **56** (2020).
18. Zarka, P. Plasma interactions of exoplanets with their parent star and associated radio emissions. *Planetary and Space Science*. **55** (5), 598-617 (2007).
19. Chin, G. et al. Lunar Reconnaissance Orbiter Overview: The Instrument Suite and Mission. *Space Science Reviews*. **129** (4), 391–419 (2007).

20. Barker, M. et al. A new lunar digital elevation model from the Lunar Orbiter Laser Altimeter and SELENE Terrain Camera. *Icarus*. **273**, 346 – 355 (2016).

21. McMullin, J. P., Waters, B., Schiebel, D., Young, W., Golap, K. CASA Architecture and Applications. *Astronomical Data Analysis Software and Systems XVI*, edited by R. A. Shaw, F. Hill, and D. J. Bell, Vol. 376 of *Astronomical Society of the Pacific Conference Series*, 127 (2007).

22. Acton, C. H. Ancillary data services of NASA's Navigation and Ancillary Information Facility. *Planetary and Space Science*. **44**, 65–70 (1996).

23. Hegedus, A. M. Data and Code Set for "Measuring the Earth's Synchrotron Emission from Radiation Belts with a Lunar Near Side Radio Array" [Data set]. *University of Michigan - Deep Blue* (2020).

24. Meyer-Vernet, N., Hoang, S., Issautier, K., Moncuquet, M., Marcos, G. Plasma Thermal Noise: The Long Wavelength Radio Limit. In *Radio Astronomy at Long Wavelengths*. ed. Stone, R.G., Weiler, K. W., Goldstein, M. L., Bougeret, J. L. American Geophysical Union (AGU). (2000).

25. Novaco, J. C., Brown, L. W. Nonthermal galactic emission below 10 megahertz. *The Astrophysical Journal*. **221**, 114–123 (1978).

26. Högbom, J. A. Aperture Synthesis with a Non-Regular Distribution of Interferometer Baselines. *Astronomy and Astrophysics Supplement*. **15** (1974).

27. Martí-Vidal, I., Pérez-Torres, M. A., Lobanov, A. P. Over-resolution of compact sources in interferometric observations. *Astronomy & Astrophysics*. 541, A135 (2012).

28. Ellingson, S.W. Sensitivity of antenna arrays for long-wavelength radio astronomy. *IEEE Transactions on Antennas and Propagation*, **59** (6), 1855–1863 (2011).

29. Crusan, J. C. et al. Deep space gateway concept: Extending human presence into cislunar space. *2018 IEEE Aerospace Conference Proceedings*. Big Sky, MT. 1-10 (2018).

30. Yushkova, O.V., Kibardina, I.N. Dielectric properties of lunar surface. *Solar System Research.* **51,** 121–126 (2017).

31. Yushkov, V., Kibardina, I., Yushkova, O. Modeling of Electrophysical Properties of the Moon Ground. *2019 Russian Open Conference on Radio Wave Propagation (RWP)*. Kazan, Russia, 463-466 (2019).

32. Burke, G., Poggio, A. Numerical Electromagnetics Code (NEC) method of moments. *Lawrence Livermore National Laboratory Technical Report* (1994).

33. Graham, S., Reckart, T. NASA-provided lunar payloads. NASA Glenn Research Center, Retrieved from https://www1.grc.nasa.gov/ space/planetary-exploration-science-technology-office-pesto/management/nasa-provided-lunar-payloads/ (2019).

Figure 1

Click here to access/download;Figure;jovefig1.pdf

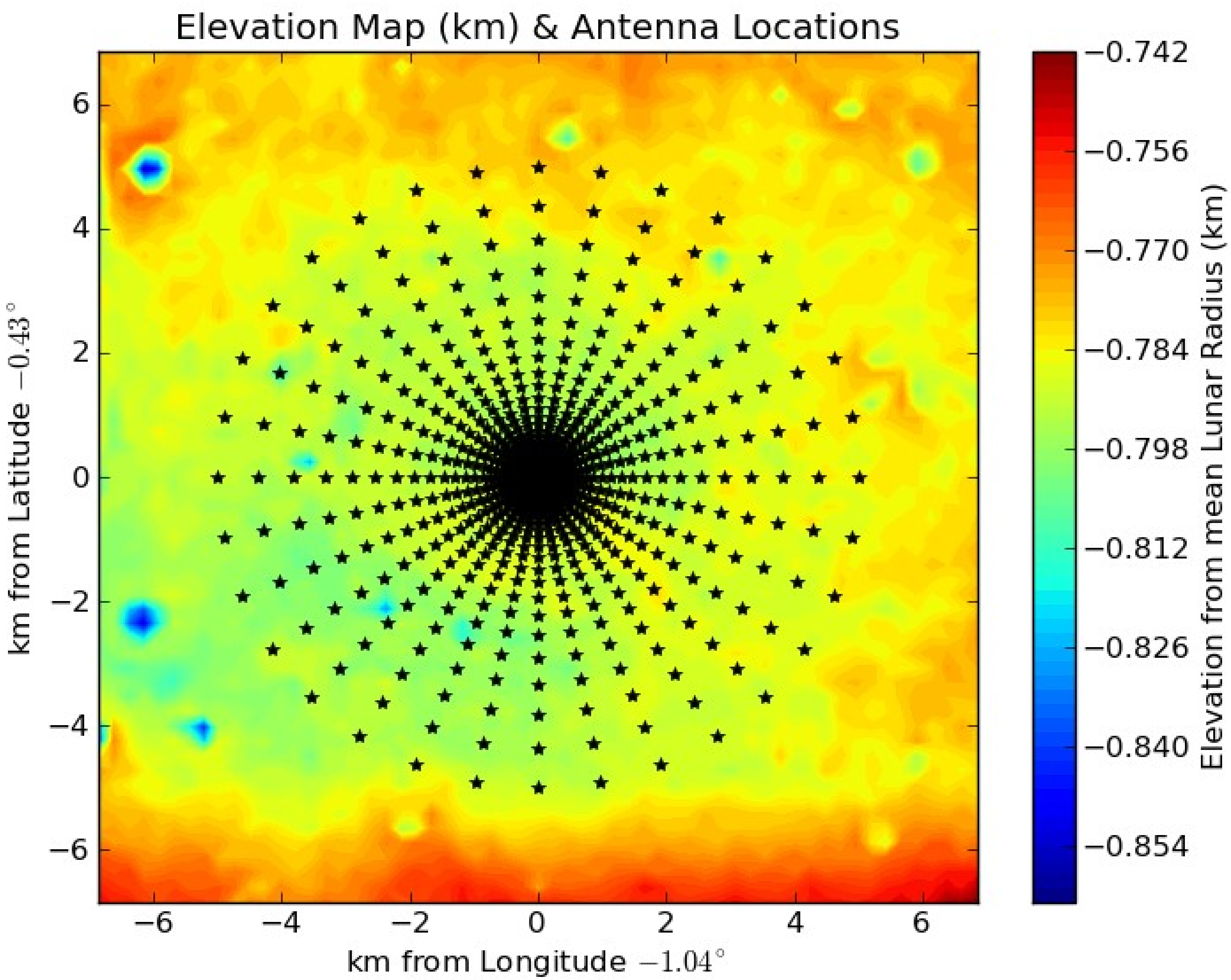

Figure 2

Click here to access/download;Figure;jovefig2.pdf

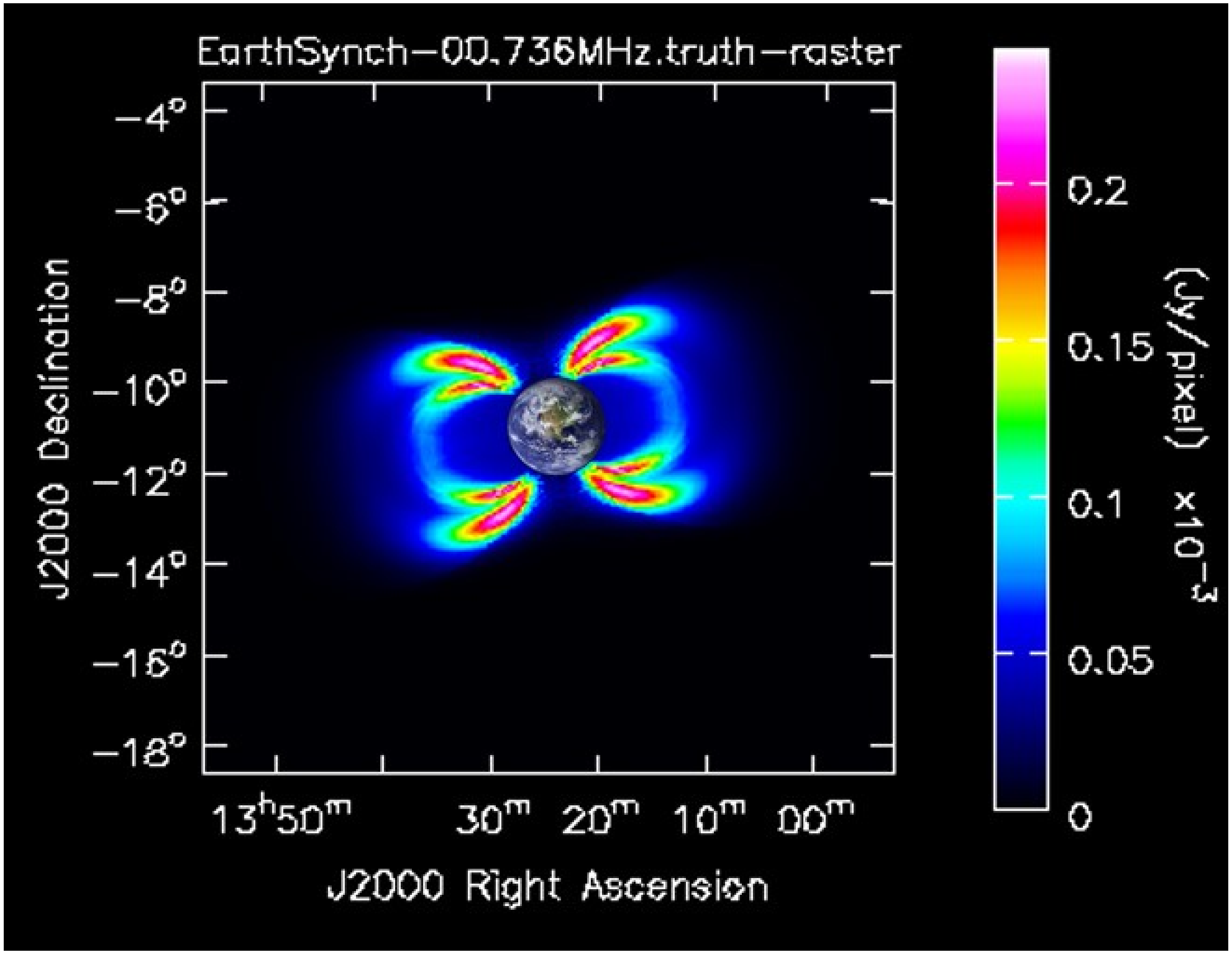

Figure 3

Click here to access/download;Figure;jovefig3.pdf

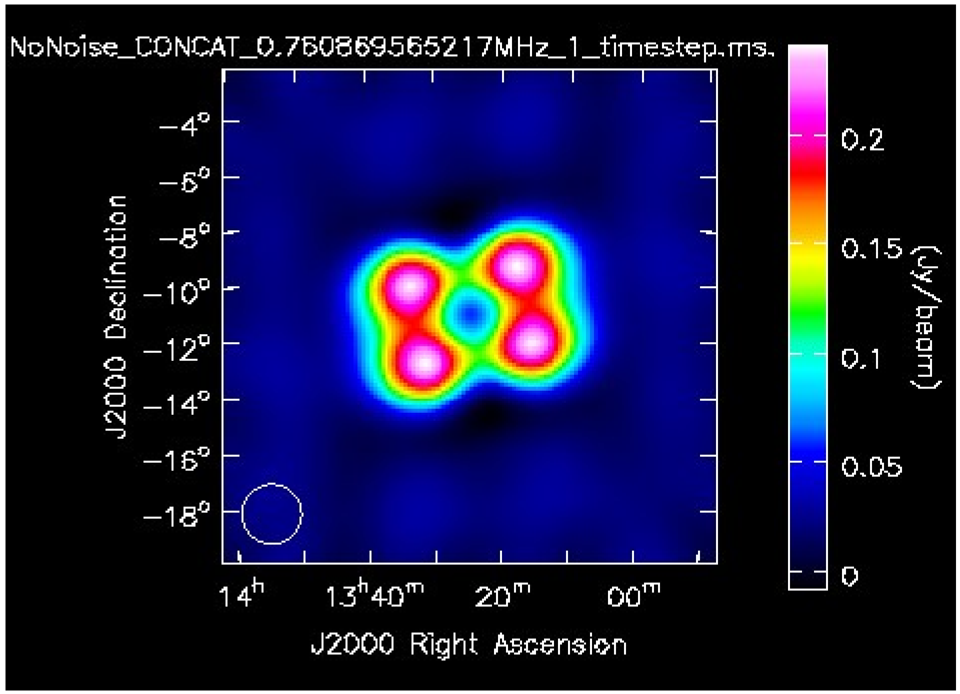

Figure 4

Click here to access/download;Figure;jovefig4.pdf

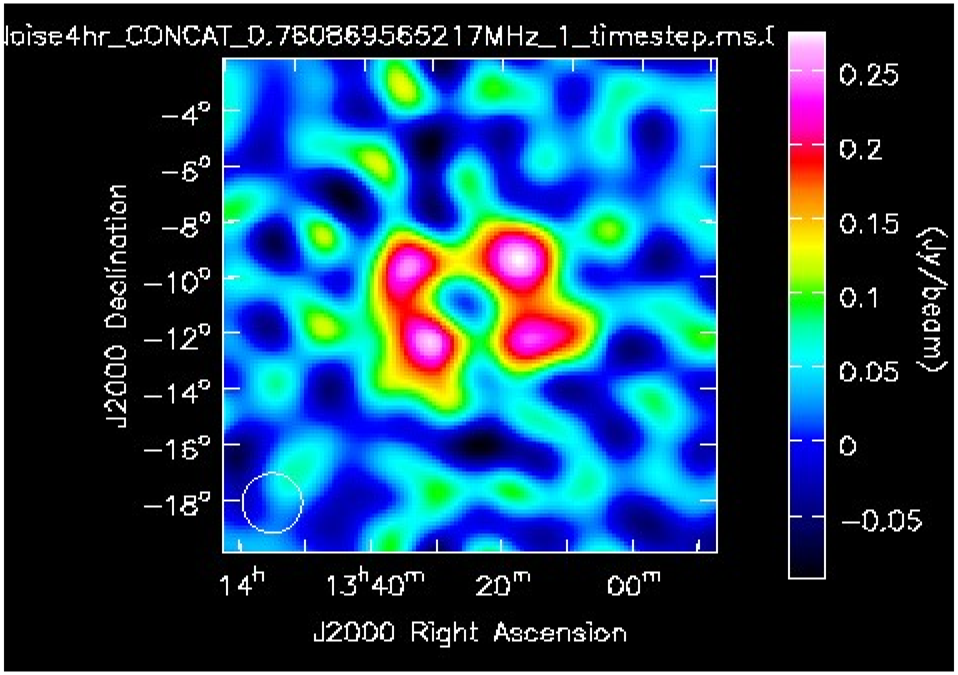

Name of Material/Equipment	Company	Catalog Number	Comments/Description
No physical materials are needed, this is a purely computational work.			

JoVE Rebuttal Document

Reviewers' comments in red

Response in black

Reviewers' comments:

Reviewer #1:

Manuscript Summary:

This manuscript describes how to simulate the imaging process of a lunar surface radio interferometer array using the software CASA, it should be useful for the design and simulation of such an array, which is currently being considered for lunar based astronomy. After clarifying two minor points the manuscript is acceptable.

Major Concerns:

(1) The author stated that in the optimal case the receiver noise dominates over the galactic background (lines 281-284). However, below 10 MHz the sky brightness temperature is very high, it may be helpful if the author could elaborate on this point a bit, e.g. what is the receiver noise temperature and the radiation power factor.

Added around line 315: "Galactic background radiation from the Milky Way (estimated by Novacco & Brown[25] to be 4.18e6 Jansky at 0.75 MHz for the full sky, of which a lunar array will only see some portion). " In that same note it is now mentioned that the electrically short dipole approximation is used, which determines the radiation power factor. The effective area is also captured in the SEFD.

(2) In line 214-215, the author says that the "Since C does not have dynamic array allocation, there was no easy way to flexibly read in the data automatically, so manual copying must be done." I am not sure what does the author mean here. Could he use malloc to generate the array of desired dimension?

Sure, in principle, one could read the file line by line and automatically determine the number of antenna by counting the lines, but one would potentially need a large buffer to hold the data you're counting to figure out how much memory you need to allocate to hold that data. Rather than that or the compromise you suggest of only changing only one variable for the number of antenna, and using that to malloc and read the data from txt files, I happened to choose to just have the user copy over the data as well. It was a design choice that probably could be better. However, the print statements from the previous python script output the data in a format easy to copy/paste into the C script. And since this code is already archived in the Deep Blue Library Archive I want to stick with working from it rather than making a near-copy and archiving that as well.

Reviewer #2:

I have read this manuscript carefully. The author focuses on simulating the response of large scale radio arrays on the Moon consisting of hundreds or thousands of antenna. In my view the novelty of the work is that it uses Digital Elevation Models from Lunar Reconnaissance Orbiter Lunar Orbiter Laser Altimeter data that allows the author to select a set of individual antenna (of array) locations for creating a synthetic aperture. However, this is not enough to design a good antenna array on the Moon.

Manuscript Summary:
OK

Major Concerns:
1) Antennas will be located on the lunar surface . It is like a semi-conductor (regolith). Moreover, the lunar surface in depth is multi-layered: dust, pieces of rock, monolith. Cosmic radio emission will penetrate into the media and be reflected, significantly affecting the array beam. It should either take this factor into account or shield your antennas from the lunar surface, making the array incredibly expensive and difficult in execution. How to lay the screen on an uneven surface? How do you imagine it, if you assumed to do so?

This issue has now been addressed in the Discussion:
"There is also the response of the lunar surface to consider. There is a layer of lunar topsoil called the regolith that acts like a lossy dielectric that can reflect incoming emission with some efficiency, above the lunar bedrock which can also reflect incoming emission with some better efficiency[30, 31]. This response is dependent on the ambient temperature and incoming frequency, as well as the chemical composition of the regolith. Studies[30, 31] have found that at lower temperatures below 100 K, the regolith is nearly transparent to radio emission, and reflection occurs at the bedrock level with a reflection coefficient of around 0.5-0.6. At higher temperatures 150-200K, the regolith can absorb emission and reflect incoming radiation at the surface with a reflection coefficient of around 0.2-0.3. At temperatures above 200 K, it is found that the dielectric properties of the regolith are diminished, and variation from reflection can be ignored. These effects can reduce the effective area of the array, reducing sensitivity and requiring longer integration times. This effect can be modeled with electromagnetic simulation software packages such as NEC4.2[32] given models of relative permittivity/dielectric constant as a function of lunar depth. This will output the SEFD of an antenna receiver for a given frequency, which can be given to the array simulation pipeline to calculate the correct noise to add to the simulated signal. Adding a grounding grid between the receiver and the lunar surface may help diminish the effect of reflected waves, but adds its own set of complications in the form of deployment."

Here I provide some estimates to the effects of the lunar surface, and point the user towards software they can use to more accurately simulate these effects for a particular receiver. All this boils down to the SEFD, so once that number is calculated one way or another, the pipeline can still use it to calculate the realistic noisy response of the array. Hopefully this is sufficient.

2) I am worried about the accuracy of the LOLA data (some meters or something like that) as applied to build a large very low-frequency array. This accuracy can be not enough. Out of phase will be accumulated in such a large array. Setting it up will be a challenge on the Moon.

This is true and a good point. It has been now been addressed in the discussion:

"Another shortcoming of this array simulation pipeline lies in the imperfect lunar surface maps used. DEMs from LRO LOLA measurements have at best a resolution of 60x60 meters/pixel in the 512 pixels/degree maps. One can interpolate these data for simulated arrays, but for real arrays there will need to be a commissioning/calibration period where sources with a known position will be used to determine the relative separations between all the antenna to high precision. Possible calibration sources include Cas A, periodic low frequency emission from Jupiter or Earth, or potentially the Lunar Gateway[29]. "

3) The author starts his presentation with the contribution of Karl G. Jansky. Of course, he is a pioneer of radio astronomy. Does he relate to radio interferometry? No. On the other hand, the author is well acquainted with the space-based experiments (WIND, STEREO), but many (well-known and interesting) design projects of antenna arrays on the Moon were overboard. Why do not they deserve to be mentioned? Introduction of this paper absolutely does not introduce the reader to the topic.

Several references have been added to the introduction outlining some of these lunar array concepts.

"Several conceptual arrays to go on the lunar surface have been drawn up over the decades. Early designs were not the most detailed, but still recognized the scientific advances that could be attained by such arrays[6, 7, 8, 9, 10]. More arrays have also been put forth in recent years, some of which, like FARSIDE[11], DEX[12], and DALI[13] seek to measure the absorption troughs of the redshifted neutral hydrogen 21-cm signal in the 10-40 MHz range to probe the so called "Dark Ages" and constrain cosmological models of the early universe. Others like ROLSS[14] call out tracking bright solar type II radio bursts far into the heliosphere to identify the site of solar energetic particle acceleration within coronal mass ejections as their compelling science case. Smaller scale arrays have also been described like the 2-element interferometer RIF[15], which would use a single lander and a moving rover to sample many baselines as it moves outward from the lander. RIF focuses on the ability to make a sky map of these low frequencies for the first time, and calculates the uv coverage and synthesized beam for integrated observations."

4) As far as I understand, this proposed antenna is intended only for studies of Earth's radiation belts so that the Earth will always be near the sky's zenith for this array. If so, this is an unjustified waste of money and resources. To fire cannons at sparrows?

Previously, the 4th paragraph of the introduction listed additional uses for lunar radio arrays. Any array with sufficient sensitivity for the Earth's synchrotron emission from its radiation belts could just as easily make similarly sensitive measurements of any of the scientific targets listed here.

In the revision, descriptions of these scientific applications have been expanded, and additional applications have been described throughout paragraphs 6 and 7 of the new introduction.

The array and its accompanying target in the form of Earth's synchrotron emission described throughout the protocol section are only meant to be an illustrative example. This is clearly a scientific extreme in terms of the low signal, but nevertheless, this pipeline allows an iterative design process to find arrays well suited for particular targets, no matter how big a cannon it ends up taking.

5) Lines 281-284: Galactic background radiation from the Milky Way makes such a big contribution in your frequency range, then others can be ignored. "This optimal noise level

assumes that amplifier noise dominates the other terms." is not a correct statement in your conditions. You cannot do this. The brightness temperature of Galactic background radiation below 10 MHz is about hundreds of thousands of degrees (K) and more. Therefore, your estimation of the antenna array sensitivity can be wrong. This means that the corresponding integration time will be other.

Added around line 315: “NOTE: For the low frequency radio regime, there are three main sources on constant noise: amplifier noise, quasithermal noise from free electrons (estimated by Meyer-Vernet et al.[24] to be 6.69e4 Jy at 0.75 MHz, using a electrically short dipole approximation), and Galactic background radiation from the Milky Way (estimated by Novacco & Brown[25] to be 4.18e6 Jansky at 0.75 MHz for the full sky, of which a lunar array will only see some portion). This optimal noise level of 1.38e7 Jy assumes that amplifier noise dominates the other terms. See Hegedus et al for a more detailed discussion. “

So I’ve shown my work a little more here, explicitly listing the calculated brightnesses that are documented in snrCalc.py. The Novacco & Brown model gives a brightness of ~3.33e5 Jy/sr, multiplied by 4pi is 4.18e6 Jy, perhaps a third to half of which will be contributing to the noise level at given time. That makes this amplifier dominated noise budget feasible, especially when you look at e.g. Zaslavsky et al 2011, which uses the Novacco & Brown model to solve for the effective length of the STEREO/WAVES antenna, and shows an amplifier noise level above anything else at 1 MHz.

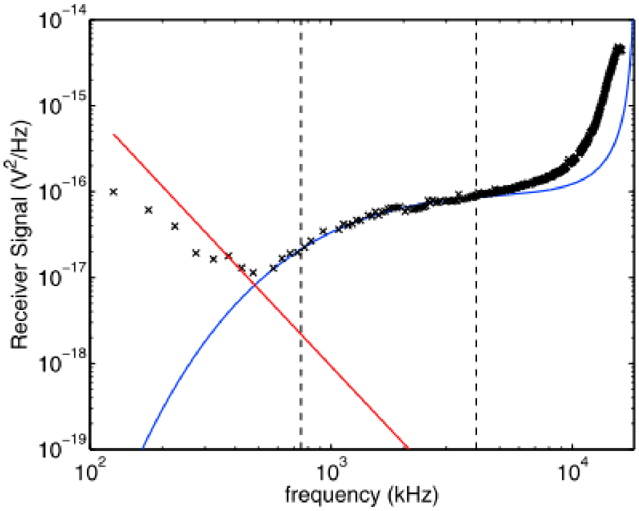

Figure 3. Receiver power spectral density $V_r^2 - V_{noise}^2$ as a function of the frequency. The black crosses are the data points obtained for the dipole XY on STEREO B. The blue solid line is the theoretical receiver power calculated from equations (11), (12), and (14). The effective length is l_{eff} = 4.30 m and the noise level is V_{noise}^2 = −162.4 dB. The red line is an approximation of the thermal plasma noise $\Gamma^2 V_{QTN}^2$, calculated from equation (6) with typical solar wind parameters n_e = 5 cm^{-3} and T_e = 10^5 K. The increase of the measured voltage spectral power at frequencies above 4 MHz (at the right of the dashed line) is the consequence of the antenna resonance discussed in the text.

Minor Concerns:
1) The author mentions the papers (lines 378 and 385) of Ellingson (2011) and (line 389) Graham & Reckart, (2019). They are absent in references.

These references have been added.

This work is too early to publish. It requires significant revision.

Reviewer #3:
Manuscript Summary:
The manuscript gives information on how to use a set of simulation tools for analyzing the effectiveness of large scale radio telescopes on the Moon. A detailed instruction on how to install the required tools is provided together with an example analysis to demonstrate how the tools work.

Major Concerns:

I have no major concerns, the description seems clear to me.

Minor Concerns:
It could be good to mention something about the required compute power for running the simulations? Is this something I can expect to run on my laptop or should I get access to a cluster for this?

A brief description of the compute time has been added in the discussion.

“These codes can all be run on an average laptop or workstation, though computation time increases with number of antenna. The slowest parts of the process are predicting the visibilities, followed by imaging. For small arrays, the entire process can be done in minutes, while for larger arrays of a few hundred or thousand receivers, hours or days may be needed. “

Reviewer #4:
Manuscript Summary:
This manuscript presents a protocol to use a computational package to simulate radio image forming on a Radio array installed on the Moon. The manuscript presents an example with imaging the Earth's magnetic field from the near side of the Moon, but it also makes clear other potential applications of this proposal for astronomical observations from the far side of the Moon.
I believe the introduction is sufficient for the purposes of the target user of this software and the different steps in the protocol are clear. It might be helpful to show how the scripts need to be edited, what variables can to be changed, in order to properly setup and customize the simulation inputs. Nevertheless, the variables are identified in the code. The code in the script files is commented and readable.

I agree, variables have been described a little better, with line numbers when appropriate. The video will hopefully capture everything nicely.

Major Concerns:
None.

Minor Concerns:
The process of customising the code in the scripts to setup the simulation needs to be clear enough. This will likely be addressed in the video, but it might be useful to list the variables

I agree, variables have been described a little better, with line numbers when appropriate. The video will hopefully capture everything nicely. I think every variable that must be changed is now mentioned by name.

JOHN WILEY AND SONS LICENSE
TERMS AND CONDITIONS

Apr 08, 2020

This Agreement between University of Michigan Ann Arbor -- Alexander Hegedus ("You") and John Wiley and Sons ("John Wiley and Sons") consists of your license details and the terms and conditions provided by John Wiley and Sons and Copyright Clearance Center.

License Number	4804490865861
License date	Apr 08, 2020
Licensed Content Publisher	John Wiley and Sons
Licensed Content Publication	Radio Science
Licensed Content Title	Measuring the Earth's Synchrotron Emission From Radiation Belts With a Lunar Near Side Radio Array
Licensed Content Author	Daniel Baker, Robert MacDowall, Baptiste Cecconi, et al
Licensed Content Date	Feb 8, 2020
Licensed Content Volume	55
Licensed Content Issue	2
Licensed Content Pages	20
Type of use	Journal/Magazine
Requestor type	Author of this Wiley article

Is the reuse sponsored by or associated with a pharmaceutical or medical products company?	no
Format	Electronic
Portion	Figure/table
Number of figures/tables	4
Will you be translating?	No
Circulation	50000 or greater
Title of new article	Simulating Imaging of Large Scale Radio Arrays on the Lunar Surface
Lead author	Alexander M. Hegedus
Title of targeted journal	Journal of Visualized Experiments
Publisher	Journal of Visualized Experiments
Expected publication date	Sep 2020
Order reference number	1
Portions	Figures 2a, 4d, 5b, 6b
Requestor Location	University of Michigan Ann Arbor 1439 Wisteria Dr ANN ARBOR, MI 48104 United States Attn: University of Michigan Ann Arbor
Publisher Tax ID	EU826007151

Total 0.00 USD

Terms and Conditions

TERMS AND CONDITIONS

This copyrighted material is owned by or exclusively licensed to John Wiley & Sons, Inc. or one of its group companies (each a"Wiley Company") or handled on behalf of a society with which a Wiley Company has exclusive publishing rights in relation to a particular work (collectively "WILEY"). By clicking "accept" in connection with completing this licensing transaction, you agree that the following terms and conditions apply to this transaction (along with the billing and payment terms and conditions established by the Copyright Clearance Center Inc., ("CCC's Billing and Payment terms and conditions"), at the time that you opened your RightsLink account (these are available at any time at http://myaccount.copyright.com).

Terms and Conditions

- The materials you have requested permission to reproduce or reuse (the "Wiley Materials") are protected by copyright.

- You are hereby granted a personal, non-exclusive, non-sub licensable (on a stand-alone basis), non-transferable, worldwide, limited license to reproduce the Wiley Materials for the purpose specified in the licensing process. This license, **and any CONTENT (PDF or image file) purchased as part of your order,** is for a one-time use only and limited to any maximum distribution number specified in the license. The first instance of republication or reuse granted by this license must be completed within two years of the date of the grant of this license (although copies prepared before the end date may be distributed thereafter). The Wiley Materials shall not be used in any other manner or for any other purpose, beyond what is granted in the license. Permission is granted subject to an appropriate acknowledgement given to the author, title of the material/book/journal and the publisher. You shall also duplicate the copyright notice that appears in the Wiley publication in your use of the Wiley Material. Permission is also granted on the understanding that nowhere in the text is a previously published source acknowledged for all or part of this Wiley Material. Any third party content is expressly excluded from this permission.

- With respect to the Wiley Materials, all rights are reserved. Except as expressly granted by the terms of the license, no part of the Wiley Materials may be copied, modified, adapted (except for minor reformatting required by the new Publication), translated, reproduced, transferred or distributed, in any form or by any means, and no derivative works may be made based on the Wiley Materials without the prior permission of the respective copyright owner.**For STM Signatory Publishers clearing permission under the terms of the STM Permissions Guidelines only, the terms of the license are extended to include subsequent editions and for editions in other languages, provided such editions are for the work as a whole in situ and does not involve the separate exploitation of the permitted figures or extracts,** You may not alter, remove or suppress in any manner any copyright, trademark or other notices displayed by the Wiley Materials. You may not license, rent, sell, loan, lease, pledge, offer as security, transfer or assign the Wiley Materials on a stand-alone basis, or any of the rights granted to you hereunder to any other person.

- The Wiley Materials and all of the intellectual property rights therein shall at all times remain the exclusive property of John Wiley & Sons Inc, the Wiley Companies, or their respective licensors, and your interest therein is only that of having possession of and the right to reproduce the Wiley Materials pursuant to Section 2 herein during the continuance of this Agreement. You agree that you own no right, title or interest in or to the Wiley Materials or any of the intellectual property rights therein. You shall have no rights hereunder other than the license as provided for above in Section 2. No right, license or interest to any trademark, trade name, service mark or other branding ("Marks") of WILEY or its licensors is granted hereunder, and you agree that you shall not assert any such right, license or interest with respect thereto

- NEITHER WILEY NOR ITS LICENSORS MAKES ANY WARRANTY OR REPRESENTATION OF ANY KIND TO YOU OR ANY THIRD PARTY, EXPRESS, IMPLIED OR STATUTORY, WITH RESPECT TO THE MATERIALS OR THE ACCURACY OF ANY INFORMATION CONTAINED IN THE MATERIALS, INCLUDING, WITHOUT LIMITATION, ANY IMPLIED WARRANTY OF MERCHANTABILITY, ACCURACY, SATISFACTORY QUALITY, FITNESS FOR A PARTICULAR PURPOSE, USABILITY, INTEGRATION OR NON-INFRINGEMENT AND ALL SUCH WARRANTIES ARE HEREBY EXCLUDED BY WILEY AND ITS LICENSORS AND WAIVED BY YOU.

- WILEY shall have the right to terminate this Agreement immediately upon breach of this Agreement by you.

- You shall indemnify, defend and hold harmless WILEY, its Licensors and their respective directors, officers, agents and employees, from and against any actual or threatened claims, demands, causes of action or proceedings arising from any breach of this Agreement by you.

- IN NO EVENT SHALL WILEY OR ITS LICENSORS BE LIABLE TO YOU OR ANY OTHER PARTY OR ANY OTHER PERSON OR ENTITY FOR ANY SPECIAL, CONSEQUENTIAL, INCIDENTAL, INDIRECT, EXEMPLARY OR PUNITIVE DAMAGES, HOWEVER CAUSED, ARISING OUT OF OR IN CONNECTION WITH THE DOWNLOADING, PROVISIONING, VIEWING OR USE OF THE MATERIALS REGARDLESS OF THE FORM OF ACTION, WHETHER FOR BREACH OF CONTRACT, BREACH OF WARRANTY, TORT, NEGLIGENCE, INFRINGEMENT OR OTHERWISE (INCLUDING, WITHOUT LIMITATION, DAMAGES BASED ON LOSS OF PROFITS, DATA, FILES, USE, BUSINESS OPPORTUNITY OR CLAIMS OF THIRD PARTIES), AND WHETHER OR NOT THE PARTY HAS BEEN ADVISED OF THE POSSIBILITY OF SUCH DAMAGES. THIS LIMITATION SHALL APPLY NOTWITHSTANDING ANY FAILURE OF ESSENTIAL PURPOSE OF ANY LIMITED REMEDY PROVIDED HEREIN.

- Should any provision of this Agreement be held by a court of competent jurisdiction to be illegal, invalid, or unenforceable, that provision shall be deemed amended to achieve as nearly as possible the same economic effect as the original provision, and the legality, validity and enforceability of the remaining provisions of this Agreement shall not be affected or impaired thereby.

- The failure of either party to enforce any term or condition of this Agreement shall not constitute a waiver of either party's right to enforce each and every term and condition of this Agreement. No breach under this agreement shall be deemed waived or excused by either party unless such waiver or consent is in writing signed by the party granting such waiver or consent. The waiver by or consent of a party to a breach of any provision of this Agreement shall not operate or be construed as a waiver of or consent to any other or subsequent breach by such other party.

- This Agreement may not be assigned (including by operation of law or otherwise) by you without WILEY's prior written consent.

- Any fee required for this permission shall be non-refundable after thirty (30) days from receipt by the CCC.

- These terms and conditions together with CCC's Billing and Payment terms and conditions (which are incorporated herein) form the entire agreement between you and WILEY concerning this licensing transaction and (in the absence of fraud) supersedes all prior agreements and representations of the parties, oral or written. This Agreement may not be amended except in writing signed by both parties. This Agreement shall be binding upon and inure to the benefit of the parties' successors, legal representatives, and authorized assigns.

- In the event of any conflict between your obligations established by these terms and conditions and those established by CCC's Billing and Payment terms and conditions, these terms and conditions shall prevail.

- WILEY expressly reserves all rights not specifically granted in the combination of (i) the license details provided by you and accepted in the course of this licensing transaction, (ii) these terms and conditions and (iii) CCC's Billing and Payment terms and conditions.

- This Agreement will be void if the Type of Use, Format, Circulation, or Requestor Type was misrepresented during the licensing process.

- This Agreement shall be governed by and construed in accordance with the laws of the State of New York, USA, without regards to such state's conflict of law rules. Any legal action, suit or proceeding arising out of or relating to these Terms and Conditions or the breach thereof shall be instituted in a court of competent jurisdiction in New York County in the State of New York in the United States of America and each party hereby consents and submits to the personal jurisdiction of such court, waives any objection to venue in such court and consents to service of process by registered or certified mail, return receipt requested, at the last known address of such party.

WILEY OPEN ACCESS TERMS AND CONDITIONS

Wiley Publishes Open Access Articles in fully Open Access Journals and in Subscription journals offering Online Open. Although most of the fully Open Access journals publish open access articles under the terms of the Creative Commons Attribution (CC BY) License only, the subscription journals and a few of the Open Access Journals offer a choice of Creative Commons Licenses. The license type is clearly identified on the article.

The Creative Commons Attribution License

Click here to access/download
Supplemental Coding Files
DeepBlueData_bg257f178.zip